Air-water Exchange of PAHs and OPAHs at a Superfund Mega-site

Lane G. Tidwell, **L. Blair Paulik**, and **Kim A. Anderson**[*]

Environmental and Molecular Toxicology Department, Oregon State University, ALS 1007, Corvallis, OR 97331
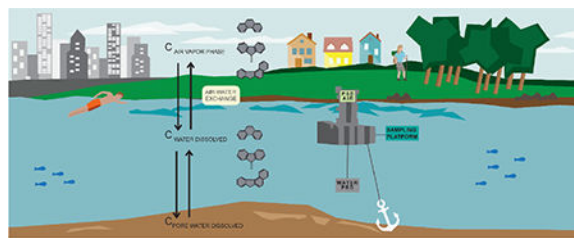
Abstract

Chemical fate is a concern at environmentally contaminated sites, but characterizing that fate can be difficult. Identifying and quantifying the movement of chemicals at the air-water interface are important steps in characterizing chemical fate. Superfund sites are often suspected sources of air pollution due to legacy sediment and water contamination. A quantitative assessment of polycyclic aromatic hydrocarbons (PAHs) and oxygenated PAH (OPAHs) diffusive flux in a river system that contains a Superfund Mega-site, and passes through residential, urban and agricultural land, has not been reported before. Here, passive sampling devices (PSDs) were used to measure 60 polycyclic aromatic hydrocarbons (PAHs) and 22 oxygenated PAH (OPAHs) in air and water. From these concentrations the magnitude and direction of contaminant flux between these two compartments was calculated. The magnitude of PAH flux was greater at sites near or within the Superfund Mega-site than outside of the Superfund Mega-site. The largest net individual PAH deposition at a single site was naphthalene at a rate of $-14,200$ (± 5780) (ng/m^2)/day. The estimated one-year total flux of phenanthrene was -7.9×10^5 (ng/m^2)/year. Human health risk associated with inhalation of vapor phase PAHs and dermal exposure to PAHs in water were assessed by calculating benzo[a]pyrene equivalent concentrations. Excess lifetime cancer risk estimates show potential increased risk associated with exposure to PAHs at sites within and in close proximity to the Superfund Mega-site. Specifically, estimated excess lifetime cancer risk associated with dermal exposure and inhalation of PAHs was above 1 in 1 million within the Superfund Mega-site. The predominant depositional flux profile observed in this study suggests that the river water in this Superfund site is largely a sink for airborne PAHs, rather than a source.

TOC art:

[*]Corresponding Author kim.anderson@oregonstate.edu, Phone: 541-737-8501, Fax: 541-737-0497.

1.0 Introduction:

Large bodies of water are often sinks for persistent organic pollutants (POP), especially PAHs (Baker and Eisenreich, 1990; Bamford et al., 1999a; Fang et al., 2012; McDonough et al., 2014; Nelson et al., 1998). Highly contaminated waters may also be sources of contaminants to air (Tidwell et al., 2016). Aquatic Superfund sites, such as the Portland Harbor Superfund Mega-site (PHSM), have long been suspected sources of air pollution (Vorhees et al., 1997). Community members and stakeholders in the vicinity of the PHSM have raised concerns about fumes and vapors arising from the Superfund site (ATSDR, 2006). It is important to characterize the environmental transport, fate and net flux of pollutants in river systems (Allan et al., 2011; Baek et al., 1991).

PAHs are pollutants that arise from natural and anthropogenic processes (Howsam and Jones, 1998). It is established that PAHs are compounds of carcinogenic concern, and more recently as compounds with non-carcinogenic health impacts, such as asthma and developmental neurotoxicity (EPA, 2010; Gale et al., 2012; Perera et al., 2009; Phillips, 1983). PAHs have long residence times in the environment, and can move between environmental compartments. Due to their persistence and potential for migration, assessing PAH flux is important when characterizing the environmental fate of these compounds.

Another class of environmental contaminants that has recently been identified as a potential concern is oxygenated PAHs (OPAHs). OPAHs are ketone or quinone-substituted PAHs (O'Connell et al., 2014). These compounds are formed through environmental transformation reactions in both air and water (Lundstedt et al., 2007). OPAHs can also be formed at the source of primary PAH production such as biomass burning or tailpipe exhaust (Jakober et al., 2007; Shen et al., 2011; Westbrook et al., 2006). The main reasons OPAHs are potentially concerning are their levels and presence in the environment, their toxicological effects in animal model systems, and their potential to generate reactive oxygen species (ROS) that may lead to disease outcomes (Chung et al., 2006; Knecht et al., 2013; O'Connell et al., 2014; Sen and Field, 2013).

The net flux of compounds at the air-water interface is the difference between its deposition and volatilization (Baker and Eisenreich, 1990). A negative flux value is defined as a

deposition, while a positive flux value is defined as a volatilization. The diffusive flux of a compound across the air-water interface is an environmental condition-controlled, compound-specific process that is driven by the inherent trend towards equilibrium between the air vapor phase and the water freely dissolved phase. The importance of understanding the diffusive flux of compounds across the air-water boundary arises from the potential for compounds to undergo any of the following: cycling between environmental compartments, transforming into more or less toxic species, and/or residing in a compartment permanently. Additionally, contamination in the respiratory zone of aquatic fauna is an important consideration for scientists assessing a contaminated ecosystem. Measuring the flux of compounds across the air-water boundary directly characterizes contaminants in these species' respiratory zone.

Assessment of flux in different systems such as remote lakes, major lake and river systems, and oceans has been performed using active sampling technologies for the last 25 years (Baker and Eisenreich, 1990; Bamford et al., 1999a; Gevao et al., 1998; Gustafson and Dickhut, 1997; Li et al., 2009; Lohmann et al., 2013). However, collecting air and water samples for flux using active sampling methods is time and labor-intensive. Diffusive flux measurement requires collecting the dissolved water fraction; utilizing active sampling necessitates actively pumping water through a filtration system (Baker and Eisenreich, 1990; Bamford et al., 1999a; Nelson et al., 1998). Air measurements require the vapor phase is collected with various filtration techniques and solid phase extractions. Active air and water sampling techniques require great care to avoid collecting particulates.

Passive sampling devices (PSDs) have been increasingly used to assess dissolved water and vapor phase air concentrations, and more recently flux (Allan et al., 2012; Allan et al., 2011; Anderson et al., 2008; Bartkow et al., 2004; Khairy and Lohmann, 2012; Matzke et al., 2012; Tidwell et al., 2016). PSDs are especially well-suited for flux assessments because they sequester the freely dissolved and the vapor phase fractions of contaminants in the water and air (Tidwell et al., 2016). PSDs are not susceptible to the bias from particulates that afflict active sampling approaches. PSDs allow for the detection of episodic events which can be missed when performing short duration active sampling. Flux has been qualitatively assessed using PSDs on a number of occasions. In each of these instances the direction of flux was calculated, but neither the rate of exchange nor the rate of mass transfer was determined (Lohmann et al., 2011; Morgan and Lohmann, 2008; Prest et al., 1995). Only two previous studies have used PSDs for quantitative assessment of diffusive flux of PAHs (McDonough et al., 2014; Tidwell et al., 2016). The limited number of quantitative studies assessing flux using PSDs shows that this application of an established technology is still in its infancy, and requires further demonstration and testing. Additionally, diffusive air-water flux in a Superfund site has never been measured. Contaminant transport and fate information is critical for performing both site and exposure assessments.

The PHSM is located on the Willamette River in Portland, Oregon. This Superfund Mega-site spans approximately 11 miles of the Willamette river. Many contaminants, including PAHs, are listed as priority concerns in both sediment and surface waters at this site (EPA, 2015). OPAHs have been measured in PHSM waters (O'Connell et al., 2014). However, to

date no information has been presented about the movement of PAH or OPAH compounds in this model system.

The objective of the present study was to use PSDs to assess contaminant fate, and estimate health risk, in and around a model Superfund site. PAH and OPAH flux was measured upriver, downriver and within the PHSM. PAH and OPAH flux were then compared, within and outside of the PHSM. Annual flux was estimated for the PHSM, and compared with the measured annual flux measured along the Louisiana coast during the Deepwater Horizon incident (Paulik et al., 2016a). Human health risk assessment (HHRA) was performed for PAH inhalation, and for dermal exposure to water in and around the PHSM. To date, no inhalation exposure HHRA has been performed for the PHSM (ATSDR, 2006; ATSDR, 2011). Estimated risk associated with inhalation exposure to PAHs within and outside of the PHSM was compared with risk during the Deepwater Horizon incident, and risks observed near natural gas extraction facilities in Ohio.

2.0   MATERIALS AND METHODS:

Study Area

The Portland Harbor Superfund Mega-site is designated as the area between river miles 1.9 and 11.8. This region contains 44 active and historic industrial sites that contributed to the legacy pollutants present in the Mega-site. There are also multiple freeway overpasses and bridges throughout this section of the river. The study area spans 18.5 river miles of the lower Willamette River in Portland, Oregon. It begins at the river's confluence with the Columbia River and ends just above its confluence with Johnson Creek (Figure 1A–1B). Air and water low density polyethylene (LDPE) PSDs were deployed from sampling platforms at five sites (Figure 1A, supplementary information Figure S2). Each sampling location was chosen in order to provide spatial resolution across the entire study area and to help highlight the potential heterogeneity while considering the river system as a single dual phase compartment. The sampling site at river mile 1 (RM 1) is downstream of the designated PHSM and has farmland on the west side of the river with a city park adjacent to a light industrial area on the east side of the river. The sampling platform at RM 3.5 is collocated with a historical point source of contamination; Ship Terminal 4 from the Port of Portland has been labeled an early action cleanup site. At this site, phase one cleanup has been completed and phase two cleanup was in planning at the time the samples were collected. RM 11 is the farthest upriver sampling site inside the PHSM. This site has heavy industrial activity on both the east and west sides of the river, and the sampling platform was adjacent to a large docking pier. Sampling at RM 12 occurred just outside the upriver boundary of the PHSM study area. At this site the sampling platform was collocated with heavy urban activities on the east and west banks of the river, and the east bank of the river also has significant traffic activity from multiple freeway overpasses. The RM 18.5 sampling site is the furthest from the PHSM study area, and it has little to no industry in the vicinity. There are a large number of residences and small businesses present on the east side of the river. At RM 18.5 wood smoke from chimneys was observed during the sampling period.

Sample Collection

Air and water samples were deployed concurrently for 17 days (September 30, 2013 - October 17, 2013) at four sites, and for 21 days (October 17, 2013 - November 7, 2013) at the fifth site. At each site, air and water cages were deployed from an anchored floating platform (supplementary information Figure S2). Sampling platform design and construction took place at the Food Safety & Environmental Stewardship laboratory. Special considerations were taken into account for changes in current, river depth, and water turbulence from boat, barge and ship traffic. For a full description, see "Sampling Platform Description" in supplementary information. Air sampler cages housed PSDs 1 meter above the water surface; these cages allowed for air circulation while minimizing sampler exposure to water, particulate deposition, and UV. Water sampler cages were suspended from the anchored platform 1 meter below the water surface; these cages provided equal flow over each PSD. Three LDPE PSDs were deployed in each air and water cage. PSDs were transported to and from sampling locations in amber glass jars. Previous work has verified that the transport times and temperatures used in this study do not affect PAH concentrations in PSDs (Donald et al., 2016). Samples were stored in the laboratory at −20°C until extraction.

PSD Preparation and Extraction

One-meter-long PSDs were constructed from additive-free LDPE tubing. Detailed PSD preparation and construction procedures are described in Anderson et al., 2008. Prior to deployment PSDs were cleaned using multiple rinses with hexanes and all PSD strips were infused with performance reference compounds (PRCs) in order to allow calculation of *in situ* air and water sampling rates (Huckins et al., 2002). The PRC compounds used can be found in supplementary information ListsS1-S2. PSDs were extracted as detailed previously (Anderson et al., 2008). Briefly, PSDs were extracted with two dialyses with n-hexane and concentrated to 1mL. Prior to extraction all samples were spiked with deuterated surrogate extraction standards to assess extraction efficiency. Surrogate extraction standards can be found in supplementary information Lists S1-S2. Extracts were stored in amber glass vials at −20°C until instrumental analysis. All solvents used were Optima® grade or better (Fisher Scientific, Pittsburgh, PA), and standards were purchased at purities 97%.

Chemical Analysis

PSD extracts were analyzed for 60 PAHs. A list of PAHs is available in supplementary information List 1. Analysis was performed using a specially equipped Agilent 7890A gas chromatograph (GC) with an Agilent 7000 GCMS/MS(Anderson et al., 2015). An Agilent Select PAH column (30m × 250μm × 0.15μm) was employed to enhance separation of compounds such as triphenylene and chrysene. GC oven parameters can be found in supplementary information. Each PAH was calibrated with a curve of at least five points, with correlation coefficients 0.98. The GC-MS/MS was operated in MRM mode. The parameters of MS/MS operation can be found in Anderson et al., 2015. A list of limits of detection (LODs) and limits of quantification (LOQs) is included in supplementary information Table S2.

PSDs were analyzed for 22 OPAHs. A list of OPAHss analyte list and physio-chemical parameters ranges is available in supplementary information List 2. OPAH analysis employed an Agilent 5975B Gas Chromatograph-Mass Spectrometer (GC-MS) with an Agilent DB-5MS column (30m × 0.25mm × 0.25μm) in electron impact mode (70 eV) using SIM. GC oven parameters can be found in supplementary information. Instrument calibration spanned 5–5000 ng-mL using a 9-point curve with a correlation coefficient > 0.98 for all target analytes. A list of LODs and LOQs is included in supplementary information Table S2.

Air-Water Flux Calculation

Environmental vapor phase air and freely dissolved water concentrations were determined using an empirical uptake model with sampling rates derived from PRC loss (Bartkow et al., 2004; Bartkow et al., 2006; Booij and Smedes, 2010; Huckins et al., 2006; Huckins et al., 2002). Water concentration calculations were described in detail in Allan et al., 2012 (Allan et al., 2012). Air concentrations are further described in Tidwell et al., 2016 (Tidwell et al., 2016). Air and water concentration equations can be found in supplementary information equations S1-S10. HOBO TidbiT® temperature data loggers were deployed with samplers in air and water.

Calculating time-weighted average environmental contaminant concentrations in both air and water allowed investigators to utilize the Whitman two-film model in order to assess the exchange and concentrations of compounds at the air-water interface. The diffusive flux of chemicals between air and water at the interface of these two environmental compartments is the movement of a chemical from the bulk phase followed by transport across the thin films of each phase into the receiving compartment bulk phase. The Whitman two-film model is used to calculate this movement:

$$\text{F} = \text{K}_{ol}(C_w - \frac{Ca}{H'_T}) \quad \text{Eq. 1}$$

where F is the flux ((ng/m^2)/day), the total mass-transfer rate coefficient is K_{ol} (m/day), and C_w and C_a are the dissolved and vapor phase concentrations in the water and air respectively (Baker and Eisenreich, 1990; Bamford et al., 1999a). Positive net flux values indicate volatilization from the water to the air; negative values denote deposition from air to water. H_T', is a dimensionless, compound-specific Henry's law value, and can be calculated using equation 2:

$$H_T' = H'_{(298)} \times e^{\frac{\Delta H_{vap}}{R} \times -\left(\frac{1}{T} - \frac{1}{298}\right)} \quad \text{Eq. 2}$$

where T is the temperature in Kelvin, $\Delta Hvap$ is the compound specific enthalpy of vaporization, and R is the ideal gas constant (8.31×10^{-3} kJ*K^{-1}*mol^{-1}). Air and water temperatures were collected hourly using temperature loggers co-located with PSDs at each sampling site. The average temperature over each deployment was used when correcting

Henry's law values for temperature. A dimensionless Henrys law value at 298 Kelvin ($H'_{(298)}$) is calculated using equation 3:

$$H'_{(298)} = \frac{H}{RT} \quad \text{Eq. 3}$$

where R is the ideal gas constant (8.2057×10^{-5} m^3 atm K^{-1} mol^{-1}) and T is the temperature in Kelvin (298). H is the Henrys law value for the compound in atm m^3/mol. The total mass transfer coefficient in equation 1 can be calculated according to equation 4:

$$\frac{1}{K_{ol}} = \frac{1}{k_a H_T'} + \frac{1}{k_w} \quad \text{Eq. 4}$$

where k_a is the air-side mass transfer coefficient and k_w is the water side mass transfer coefficient. Compound specific diffusivity values for 60 PAHs and 22 OPAHs in water (D_{iw}) were calculated from the molecular weight of each compound based on the relation defined previously (Schwarzenbach et al., 2002). D_{iw} were used to calculate Schmidt values as inputs for water-side mass transfer coefficients. The air-side mass transfer coefficients were calculated by scaling the wind speed at ten meters above the water surface with the molecular weight of the compound to the CO_2 diffusivity and the temperature-corrected Henry's law value. Further details of the calculations are described elsewhere (Bamford et al., 1999a; Johnson, 2010; Tidwell et al., 2016). PSDs were used to sample vapor phase and freely dissolved concentrations in air and water.

Concentrations in the environment derived from PSDs represent the time-weighted average concentrations over the course of the deployment period. The flux described in this work is the time-weighted average net flux over each sampling period. Wind speed as well as air and water temperature were collected in real-time over the course of each sampling period. Averaged temperature and wind speed inputs were used in the time-weighted average flux calculations, Eq. 1 and subsequent inputs. Error estimates shown for each net flux value in supplementary information Table S1 in the column labeled pooled variance represents the variance of flux from n=3 air and water replicates deployed at two sites (one inside and one outside the Superfund site). The difference in magnitude of flux based on the triplicate error assessments was all less than 30%. The highest of average error found at replicate sites for each compound was then applied to the remaining sampling sites' data. Applying additional uncertainties to mass transfer values applied to averaged values was determined to be an overly conservative approach. In instances where an analyte was below the LOD in one or both environmental compartments, net flux was estimated by calculating the environmental concentration from a value of one half the instrumental LOD as was done in a previous study (McDonough et al., 2014). Net mass transfer coefficients, wind speeds, and air and water temperatures are shown in supplementary information Table S1.

PAH Source Apportionment

PAH isomer ratios have been used to identify point sources for over 30 years (Daisey et al., 1979; Esen et al., 2008; Galarneau, 2008; Nielsen, 1996). We used a set of isomer ratios to differentiate between pyrogenic and petrogenic sources. Anthracene/(anthracene +phenanthrene) ratios <0.1 indicate petrogenic sources and ratios >0.1 indicate pyrogenic sources (Pies et al., 2008; Tobiszewski and Namiesnik, 2012; Yunker et al., 2002).

Fluoranthene/(fluoranthene+pyrene) ratios 0.5 indicate pyrogenic sources, and ratios 0.4 indicate petrogenic sources (Tobiszewski and Namiesnik, 2012; Zhang et al., 2008). For the fluoranthene/(fluoranthene+pyrene) ratio, Yunker et al., 2002 suggests that values between 0.4 and 0.5 indicate liquid fossil fuel combustion (Yunker et al., 2002).

Data analysis

Differences between sites were assessed by Wilcoxon rank-sum tests using R version 2.15 software. Differences were considered significant at a probability value of p 0.05.

Quality Control

Quality control (QC) samples accounted for over 35% of the total number of samples analyzed, and included: PSD preparation blanks, field and trip blanks for each deployment and retrieval trip, post-deployment cleaning blanks and laboratory reagent blanks. Analyte concentrations found in QC samples were subtracted from instrumental concentrations found in environmentally-deployed PSDs. With the exception of naphthalenes all corrections from concentrations in blank samples resulted in 12% or less correction to final environmental calculations. Naphthalene and 1-methylnaphthalene corrections ranged between 20–50% and 10–30% respectively. PAH and OPAH extraction surrogates were added to all samples immediately prior to PSD extraction. PAH concentrations were surrogate recovery-corrected during instrumental analysis. OPAH concentrations were not surrogate recovery-corrected during instrumental analysis. However, extraction surrogates were employed to calculate percent recoveries, listed below. For both air and water, the mean extraction surrogate recoveries were 50% for naphthalene-d8, 51% for acenaphthylene-d8, 75% for phenanthrene-d10, 82% for fluoranthene-d10, 93% for chrysene-d12, 97% for benzo[a]pyrene-d12, 92% for dibenzo[g,h,i]perylene-d12, 71% for 9-fluoronone-d8, 47% for 2-methyl-l,4-naphthalenequinone-d8. The average relative percent difference of Σ_{60}PAH in air sampling field replicates was 21%. Average relative percent difference of Σ_{60}PAH in water sampling field replicates was 17%. Relative percent differences of Σ_{22}OPAH in air sampling field replicates was 20%. Average relative percent differences of Σ_{22}OPAH among water sampling field replicates was 2%. Field replication was done in triplicate at one site inside and one site outside of the PHSM.

Human Health Risk Assessment

Quantitative human health risk assessment was used to estimate carcinogenic risks associated with inhalation exposure to vapor phase PAH mixtures in air, and dermal exposure arising from recreational activities in water containing PAH mixtures at each site. Specifically, each individual PAH concentration was multiplied by its relative potency factor (RPF) assigned by the U.S. EPA, yielding a benzo[a]pyrene equivalent concentration

(B[a]Peq) (EPA, 2010). A list of RPF values for each PAH that has a potency factor associated with it is shown in supplementary information Table S3. B[a]Peq was used to estimate excess lifetime cancer risk associated with this exposure. The excess lifetime cancer risk (ELCR) estimate can be defined as a probability of the maximum number of potential cancer cases observed above background that is associated with a given exposure. ELCRs can be compared to an acceptable risk level (defined by the EPA as a range from one in 10,000 to one in 1,000,000) for a given exposure, to determine whether exposure to measured levels of pollutants might be concerning (ATSDR, 2006; EPA, 2005). In this work, an increased ELCR is defined by the authors as a probability or maximum risk exceeding 1 in a million. Risks were estimated for residential and occupational "outdoor worker" exposure scenarios for the inhalation pathway and recreational swimmer and recreational angler for dermal exposure to water. Risk estimates were calculated as defined by the U.S. EPA and the U.S. Agency for Toxic Substances and Disease Registry (ATSDR)'s recent Public Health Assessment for this site (ATSDR, 2011; EPA, 2014). In all exposure scenarios the average lifetime was set at 78 years. For the residential inhalation scenario, 26 years was used as the exposure duration and the exposure frequency was set at 350 days per year, with a daily exposure of 24 hours. In the outdoor worker inhalation scenario, 225 days per year, 25 years, and 8 hours per day were used for exposure frequency, exposure duration and daily exposure, respectively. The inhalation unit risk (IUR) value used for inhalation risk assessment was 8.7×10^{-5} ng/m^3 (WHO, 2000). For dermal exposure for recreational anglers and swimmers, the exposure frequency was set at 26 and 156 days per year, respectively, with exposure duration of one hour per day for 30 years. Surface area of exposed skin was set at and 1980 cm^2 for the angler scenario and 19,400 cm^2 for the swimmer scenario (ATSDR, 2011). All risk estimates assume exposed individuals are adults. Risk assessment equations are listed in supplementary information equations S11-S15. All other exposure factors used in this risk assessment are also defined in supplementary information.

3.0   RESULTS AND DISCUSSION

PAH and OPAH levels in Air and Water

Σ_{60}PAH vapor phase concentrations increased at each site from RM 1 through RM 12, (Figure 2C). The four PAHs that contributed most to Σ_{60}PAH at all sites were naphthalene, acenaphthene, fluorene and phenanthrene, contributing 28–52%, 19–23%, 3–8%, and 1–5% respectively (supplementary information Figure S4). Phenanthrene concentrations in air at RM 12 were three times higher than the highest phenanthrene concentrations observed in a previous study using LDPE to sample air near the population center of Cleveland, Ohio (McDonough et al., 2014). Phenanthrene levels at RM12 were twice as high as the highest). Σ_{60}PAH concentrations were 33 times higher at RM 12 than in a study where LDPE was employed to sample air within a tenth of a mile of hydraulic fracturing natural gas well pads (Paulik et al., 2016a). It is not surprising that PAH concentrations in the PHSM are higher than near natural gas extraction in rural areas of Ohio, where overall background PAH concentrations may be lower. However, it is somewhat surprising that PHSM PAH levels are higher than those found by McDonough et al., in Cleveland, Ohio (McDonough et al., 2014). Cleveland is a city of a similar size as Portland, but it is in a much more industrially

developed area. However, the proximity of the Cleveland sampling sites to the great lakes' large air masses is possibly contributing to dilution of the PAHs from industrial point sources.

Diagnostic isomer ratios showed evidence of pyrogenic sources at RM 12 (supplementary information Figure S2). This is consistent with the site being located directly beneath the U.S. interstate 5 freeway overpass. All sites showed pyrogenic signatures in air, however sites RM1 through RM 12 showed pyrogenic signatures that are consistent with fossil fuel combustion, while the site at RM18.5 showed evidence of a wood combustion source. The distance between U.S. interstate 5 and each sampling site was investigated to attempt to identify it as a potential significant point source of vapor phase PAHs. Differences between isomer ratios at the four downriver sampling sites and RM 18.5 were not indicative of the freeway being the only major point source of pyrogenic PAHs. While RM1 through RM12 all share similar PAH isomer ratios the distance measured in a straight line from sampling sites to U.S. interstate 5 ranges between 5.2 miles at RM 1 to 0.012 miles at RM 12, while RM 18.5 is located 2.7 miles from the freeway (supplementary information Table S5). This suggests that while U.S. interstate 5 does likely produce significant PAH pollution it is not the only major source contributing vapor phase PAHs to the PHSM. In Paulik et al., 2016 PAH isomer ratios suggested that PAH mixtures showed a predominantly petrogenic signature, which is consistent with PAHs coming from fugitive emissions during natural gas extraction activities (Paulik et al., 2016a). In contrast, PAHs detected at RM 12 showed evidence of more pyrogenic or mixed signatures, suggesting these PAHs may come from tail pipe exhaust from the highway overpass, boat and barge traffic on the river, or from industrial practices (supplementary information Figure S2).

Σ_{22}OPAH air concentrations were five orders of magnitude lower than Σ_{60}PAH air concentrations at all sampling sites (Figure 2C). This is likely due to the shorter OPAH analyte list, and the more semi-polar nature of OPAHs. The semi-polar nature of OPAHs makes them more likely than PAHs to partition into the aqueous compartment in greater quantities. Σ_{22}OPAH air concentrations were highest at RM 12 and RM 3.5 (Figure 2C). Σ_{22}OPAH air concentrations at both of these sites were 200–500 times smaller than the two largest Σ_{22}OPAH air concentrations measured during the Deepwater Horizon incident in the Gulf of Mexico in a previous study (Tidwell et al., 2016). It is important to note that high OP AH concentrations were recorded during the Deepwater Horizon incident (DWH) shoreline oiling events. The DWH sample may therefore be a high estimate of Σ_{22}OPAH air in the Gulf of Mexico on average. All other Σ_{22}OPAH air concentrations measured in the DWH study were within an order of magnitude of those measured in the PHSM in this study (Tidwell et al., 2016). The OP AH that contributed most to Σ_{22}OPAH at the two sites with the highest Σ_{22}OPAH in the PHSM was acenaphthenequinone, contributing 65% at RM 3.5, and 81% at RM 12 (supplementary information Table S1, Figure S3).

The sources of OPAHs may be linked to their parent PAHs found at each site. Acenaphthene is one of the most abundant PAHs at RM 12, and it is an environmental precursor to acenaphthenequinone (supplementary information Table S1). Benzofluoreneone was detected at four of the five sampling sites, with the highest concentration observed at RM 12 $(1.14 \times 10^{-4}$ $(\pm 3.1 \times 10^{-5})$ ng/m^3) (supplementary information Table S1). This finding is an

order of magnitude lower than benzofluoreneone air concentrations commonly detected in Gulf of Mexico air sampled during the DWH incident (Tidwell et al., 2016). Air concentrations of benzofluoreneone in the PHSM were significantly lower than vapor phase concentrations observed by Albinet et al., 2007 in the Marseille region of France, which encompassed suburban and industrial/urban regions similar to those found at sampling sites in this study (Albinet et al., 2007). Given this similarity in sampling sites, and that both techniques focused on vapor phase concentrations, the lower concentrations of benzofluorenone across the PHSM may be explained by lower concentrations of PAH precursors. Another potential explanation for the difference in concentrations could be the result of precursor PAHs undergoing different environmental transformation pathways in and around the PHSM resulting in different environmental degradation products.

Freely dissolved PAHs in water showed the opposite spatial trend compared to air. In water, Σ_{60}PAH concentrations were higher downstream at RM 3.5 and RM 1 than at upstream sites (Figure 2D). Elevated levels of 20 ($\pm$4) ng/L at RM 3.5 are similar to those observed in the PHSM during July and August of 2010 (Matzke et al., 2012). Major PAHs contributing to the sum concentration at both RM 1 and RM 3.5 were phenanthrene, pyrene and 2,3-dimethylanthracene. However, it is important to note that the number and frequency of PAH detections at all sites is higher in water than in air in this study (supplementary information Table S1). One possible explanation for the detection frequency in water may be legacy PAH contamination in sediments that are released over time, while PAHs in air may be predominantly from contemporary sources (Sower and Anderson, 2008). Further research on the flux of PAHs between sediments and water, and aquatic transformation reactions such as oxygenation of PAHs, is warranted to answer these questions.

Σ_{22}OPAH water concentrations were an order of magnitude higher than Σ_{60}PAH concentrations. The highest Σ_{22}OPAH concentration in water was 279 ($\pm$17) ng/L, measured at RM 1. OPAH concentrations at this site were significantly elevated compared to all other sites (p 0.05). A high degree of variability in OPAH detection frequency and Σ_{22}OPAH concentrations in water was observed throughout the river system. The sample collected at RM 11, located inside the Superfund study area, had only one OPAH detected above LOQs. As a result of the single detection and the relatively low abundance, this site was significantly different from all other sites (p 0.01) (Figure 3D, supplementary information Table 1). RM 12 and RM 18.5 had similar Σ_{22}OPAH water concentrations, and acenaphthenequinone contributed greater than 50% to the total mass of OPAH measured at both sites. Σ_{22}OPAH in water at RM 3.5 was 4.5 times higher than in the PHSM during 2011 (O'Connell et al., 2014). This increased level of OPAHs in water, during the same season but two years later, may be evidence of an episodic event occurring at this site while the samplers were deployed. The primary OPAH driving the total OPAH concentrations in the O'Connell et al. study was 9,10-anthraquinone. The 9,10-anthraquinone is primarily derived from anthracene, which was measured in moderate to low concentrations during the O'Connell study (Mallakin et al., 2000; O'Connell et al., 2014). However, the primary contributor to the high total OPAH water concentration during the 2013 sampling was acenaphthenequinone, which can arise from a variety of parent PAHs including acenaphthene and acenaphthylene (Selifonov et al., 1996). Both of these PAHs were measured in water at this site, but not at concentrations significantly different than other sites

(supplementary information Table S1). This result is consistent with the hypothesis of an upstream event and subsequent environmental transformation, such as a biogenic or ultraviolet-induced transformation, occurring while the compounds were transported downstream.

PAH and OPAH Flux

Understanding the movement of persistent organic pollutants in complex river systems is important for assessing the source and environmental fate of these compounds. This information will improve exposure estimates for use in both human health and ecological risk assessments. The majority of PAHs that were detected in both environmental compartments were moving from air to water. Specifically, 16 of these 26 PAHs were in states of deposition at all five study sites during the sampling period. This suggests that the PHSM was mainly acting as a sink for air pollutants rather than a source. This is notable, as it is typically expected that sites of legacy contamination like the PHSM may be a major contributor of pollution to the surrounding area's air.

Naphthalene had the greatest magnitude of both volatilization and deposition in this study. Naphthalene flux changed direction from volatilization to deposition within the PHSM and remained in deposition until RM 18.5, where volatilization was occurring, but at significantly lower levels than those seen at RM 3.5 and RM 1 (Figure 2A, supplementary information Table S1). The magnitude of phenanthrene depositional flux tripled moving upriver from RM 1 to RM 11. The phenanthrene deposition peaked at $-2,180$ (± 330) (ng/m^2)/day at RM 11 (Figure 2A, Supplementary information Table S1). Phenanthrene deposition decreased slightly to a rate of $-1,580$ (± 320) (ng/m^2)/day at RM 12. It then significantly decreased at RM 18.5, which is the sampling site six miles upriver of the PHSM (Figure 2A). Phenanthrene deposition at RM 11 was two times greater than the highest deposition rates observed by McDonough et al., in a study performed on the Great Lakes near numerous population centers (McDonough et al., 2014). The difference in magnitude of depositional flux of phenanthrene between the Great Lakes region and the PHSM is likely due to the increased air and water mass present in the Great Lakes. The Great Lakes air and water masses may dilute PAHs emitted from population centers in McDonough et al. In contrast, the sampling sites in the present study were either within or very close to the city of Portland, which is located over 100 miles from the Pacific Ocean. Portland is also protected by geological formations that result in decreased potential for dilution from large air mass exchange. Another potential factor contributing to the differences observed between these two studies was the generally lower ambient air temperatures in PHSM during the same sampling season. Cooler air temperatures result in increased deposition from the vapor phase, which would be consistent with increased deposition in the Willamette River in the PHSM (Bamford et al., 1999b).

While the magnitudes of depositional flux of other PAHs were smaller than that measured for naphthalene, 3 and 4-ring PAHs in this study were also actively exchanging across the air-water boundary. Anthracene, fluorene, acenaphthene all followed a similar profile of depositional increase from RM 1 to RM 12, with a significant decrease in deposition at RM 18.5 (supplementary information Table S1). Pyrene was in deposition at RM 11 and 12 and

in volatilization at all other sites. Acenaphthene was in a deposition phase at all sites in this study and had the second largest flux magnitude (Figure 3A). This is in contrast to an investigation in an industrialized harbor in Taiwan, performed by Meng-Der Fang et al., 2012, which observed acenaphthene flux in volatilization during the months of September and October (Fang et al., 2012). This difference may be explained by the different seasonal weather patterns between these two sampling sites. September and October are the monsoon season in Taiwan, where daily rain events scrub the air of PAHs and replenish the water mass, resulting in high water concentrations and low air concentrations that give rise to the general trend of volatilization (Fang et al., 2012). The PHSM is characterized by extended dry periods during this time of year. These dry conditions would be expected to result in periods of steady state or light deposition, however large depositional mass transfers occurred. This discrepancy suggests that the continual input of PAHs into the atmosphere from anthropogenic activities in the PHSM is promoting this large depositional paradigm.

Four-ring PAHs in the family of benzo[x]fluorene had different flux profiles than either pyrene or 3-ring PAHs like phenanthrene and fluorene. Net mass transfer for benzo[a], benzo[b] and benzo[c]fluorene was estimated to be at, or close to, steady state at RM 1, RM 3.5 and RM 18.5. However, deposition from air to water of the benzo[x]fluorene family was observed at RM 11 and RM 12 (supplementary information Table S1). Benzo[c]fluorene is a carcinogen, and is of particular interest as the concentrations in air and water results in deposition at -1.29×10^{-1} ($\pm 2.5 \times 10^{-2}$) (ng/m^2)/day and -2.23×10^{-1} ($\pm 2.1 \times 10^{-2}$) (ng/m^2)/day at RM 11 and RM 12, respectively. The carcinogenicity of benzo[c]fluorene is discussed below.

The estimated 12-month net flux of phenanthrene in the PHSM at the site with the largest deposition (RM 11) was -7.9×10^5 (ng/m^2)/year. A previous study, using the same techniques, in response to the Deepwater Horizon incident measured 12-month net flux for phenanthrene in Louisiana at 0.13×10^5 (ng/m^2)/year (Tidwell et al., 2016). The measured 12-month mass transfer of phenanthrene in an industrial harbor in Taiwan was approximately -400 (ng/m^2)/year (Fang et al., 2012). The Taiwan study takes into account the cancellation effect of having seasonal cycles of deposition and volatilization, which can nullify large mass transfers over the course of the year. We sampled in the driest season, which would potentially bias our sampling event toward conditions that typically favor deposition. Cool and wet environmental conditions scrubs the air and would result in increased water concentrations and conditions that promote volatilization (Fang et al., 2012). However Gustafson and Dickhut found phenanthrene in deposition on both the York River and the Elizabeth River in the USA during the cool rainy season (Gustafson and Dickhut, 1997). Given the similarities in site characteristics between the PHSM and the York and Elizabeth Rivers, it is reasonable that phenanthrene is also in deposition during the cold and raining seasons in the present study. It can further be speculated that the PHSM may not have significant changes in flux direction in different seasons. This suggests that this site has significant mass transfer from the activities taking place in and around the PHSM area into the river. Further assessment of seasonal effects on flux in this system is warranted. Most importantly, it should be noted that the Willamette River acts as a large sink for PAHs, rather than a source, both within and outside the PHSM area during this study period.

The spatial profile of OPAH net flux was quite different than that of PAHs (Figure 3B). All OPAHs that were detected in both environmental compartments were in a state of volatilization or at steady state at all sampling sites. Rates of volatilization for acenaphthenequinone decreased from RM 1 (411 ($\pm$20) (ng/m^2)/day) to RM 3.5 (110 ($\pm$3) (ng/m^2)/day), and then further decreased to a rate of approximately 20 (ng/m^2)/day for all other sites (Figure 3B). Rates of volatilization for 1,4-anthraquinone decreased from RM 1 (42 ($\pm$20) (ng/m^2)/day) to RM 11 where near steady state was observed, followed by increased rates that were not significantly different from RM 1 at upriver sites RM 12 and RM 18.5 (Figure 3B).

An important consideration when using PSDs to assess flux is the time-weighted-average concentrations that the samplers yield. The flux calculated for the PHSM in this study represents the average net flux over the entire deployment period. While this can be interpreted as a positive aspect of this type of assessment, it is important to recognize that some information may also be lost using this approach. For instance, short-term changes in flux direction or magnitude may be detected with active sampling techniques using shorter time periods, but would be masked when using a PSD that is deployed for days to weeks at a time. PSDs sequester the vapor phase and freely dissolved fractions of compounds in the air and water, respectively. This phase-specific sequestration makes PSDs especially well-suited for assessment of the diffusive exchange of compounds at the air-water interface. However, it is important to note that the diffusive exchange is not the only type of mass transfer that can occur at the air-water boundary layer. Deposition of wet and dry particles may also contribute to the total flux of a system, and should be considered when estimating total contaminant transport. Because these two types of deposition are not accounted for in this study, the results presented here may represent an underestimation of the total deposition of PAH and OPAH to PHSM waters.

Human Health Risk Assessment for Exposure to PAHs via Inhalation and Dermal Contact with Water

The carcinogenic potency of PAH mixtures in air was significantly higher at RM 11 and RM 12 than at other sampling sites, with B[a]P$_{eq}$ concentrations of 0.0599 ($\pm$0.004) ng/m^3 and 0.0593 ($\pm$0.004) ng/m^3, respectively (Figure 3A). Both of these sites are in the heavily urbanized/industrialized area of Portland Harbor. RM 11 is inside the PHSM, and RM 12 is just upriver of the PHSM boundary, but adjacent to heavy automobile traffic (Figure 1). The predominant PAH elevating B[a]P$_{eq}$ at both of these sites is benzo[c]fluorene (supplementary information Table S1). B[a]P$_{eq}$ concentrations in water were highest at RM 3.5, and benzo[c]fluorene was also the PAH contributing the greatest carcinogenic equivalence at this river mile. Benzo[c]fluorene was assigned an RPF of 20 in the EPA's 2010 guidance document (EPA, 2010). This suggests that benzo[c]fluorene is 20 times more carcinogenic than benzo[a]pyrene. Thus, even a small concentration of benzo[c]fluorene can dominate the estimated carcinogenic potency of a PAH mixture when the EPA's 2010 RPFs are used. No sampling site exceeded a waterborne B[a]P$_{eq}$ concentration of 1 ng/L (Figure 3D). Additionally, increased B[a]P$_{eq}$ concentrations were observed in water at sites downriver of sites with the highest B[a]P$_{eq}$ in air. This suggests that benzo[c]fluorene in air is deposited into the water and contributes to B[a]P$_{eq}$ at sites downriver.

Inhalation-based estimated excess lifetime cancer risk (ELCR) for individuals working outdoors at RM 11 and RM 12 were 0.38 and 0.37 in one million, respectively. Both of these values are below the most conservative level of concern (Figure 3B). Inhalation-based ELCR estimates are higher for residentially exposed individuals: 1.86 and 1.84 in one million for RM 11 and 12, respectively (Figure 3C). Occupational risk estimates at these two sites are 46 times higher than risk estimates at sites adjacent to hydraulic fracturing natural gas wells (Paulik et al., 2016b). Residential risk estimates are 1000 times higher than the risk estimated near natural gas extraction activity (Paulik et al., 2016b). The estimated inhalation risk at the downriver PHSM site (RM 3.5) was not significantly different than the site upriver of the PHSM (RM 18.5). The estimated human health risks associated with RPF-based PAH inhalation during the Deepwater Horizon incident never exceeded the probability of 1 excess cancer in one million individuals, even during shoreline oiling events in Grand Isle, Louisiana(Tidwell et al., 2016). This suggests that, even during major environmental disasters, inhalation risk may actually be lower for individuals in close proximity to spills than for individuals residing in, or working near, everyday industrial or other anthropogenic activities that emit PAHs year round. In the case of the Deepwater Horizon, we speculate that contaminant concentrations in Louisiana air were heavily diluted by the large Gulf of Mexico air mass (Tidwell et al., 2016). It is important to note that the sampling site with the second highest lifetime cancer risk calculated in both inhalation paradigms in the present study (RM 12) is just upriver of the PHSM's upper boundary. While legacy pollution plays an important role in human health risk, exposure to modern anthropogenic activities (such as heavy traffic from freeway overpasses at RM 12) also has substantial potential to negatively impact human health. No prior assessment of increased ELCR attributed to inhalation exposure in the PHSM has been performed (ATSDR, 2011). Thus, it is an important finding that risk estimates associated with inhaling vapor phase PAHs were relatively low.

The greatest estimated ELCR for dermal exposure to water while swimming was measured at RM 3.5 (Figure 3E). Similar to the inhalation exposure pathway, benzo[c]fluorene was the PAH contributing most heavily to estimated carcinogenic risk from skin contact with water at this site. The estimated ELCR at RM 3.5 for dermal water exposure for anglers exceeded the 1 in one million baseline level, but was an order of magnitude lower than ELCR estimated for a swimming exposure (Figure 3.3F).

The U.S. ATSDR performed a Public Health Assessment (PHA) for PHSM in 2006, assessing cancer risk associated with PAH exposure through fish consumption and dermal exposure to river water and sediment.(ATSDR, 2006; ATSDR, 2011) It is unclear in the 2011 ATSDR Final Release PHA whether the freely dissolved fraction or the total PAH (freely dissolved plus particulate-bound) concentration was used to assess carcinogenic risk related to dermal exposure. The PSDs used in this study sequester only the freely dissolved fraction of PAHs in water, which is considered the bioavailable fraction (Greenberg et al., 2014). The highest estimated ELCR for recreational swimmers in this study is 1.5 time greater than the carcinogenic risk estimated by the ATSDR in 2011 (Figure 3E, supplementary information Table S4) (ATSDR, 2011). This discrepancy is likely due to the expanded list of PAHs assessed in this study, and the high carcinogenic potencies of some of these PAHs on the EPA's 2010 RPF list (EPA, 2010). Given these methodological

differences, this difference should not be interpreted as an increase in carcinogenic PAH concentrations in the river system between the years of 2011 and 2013.

A direct comparison of the seven PAHs used to assess carcinogenicity in the ATSDR PHA and measured in the present study is in supplementary information Table S4. Similar to the 2011 ATSDR PHA, no individual carcinogenic PAH exceeded the baseline level of concern in this study. However, when comparing the sum of the same seven PAHs used in the ATSDR 2011 PHA and this study, RM 3.5 and RM 1 exceeded the 1 in one million baseline level of concern set in this study (supplementary information Table S4).

Risk Assessment Limitations

There are many uncertainties inherent in risk assessment. These include extrapolating from a relatively short sampling period to a lifetime of exposure, making assumptions about exposure duration and frequency, and extrapolating from stationary sampling data to the exposure of mobile humans. These uncertainties are not unique to the risk estimate in this study. However, they should be taken into consideration when interpreting its findings. Exposure factors estimating exposure frequency and duration were estimated based on U.S. EPA and ATSDR guidance (ATSDR, 2011; EPA, 2014). It should be noted that changing any one of these factors can substantially affect risk estimates. For instance, the residential inhalation risk assessment assumes exposure occurs for 26 years. This assumes that exposed individuals live near the measured PAH levels for the majority of their adult lives. If it were instead estimated that exposure only occurred for one year, risk estimates would decrease by a factor of 26. This could substantially change the interpretation of potential risk.

It should also be considered that PAH levels in this risk assessment were measured for a few weeks of the year. The risk assessments, however, assume that exposure occurs consistently for 25–30 years. There is potential for PAH levels to vary with seasonal changes, and from year to year (Sower and Anderson, 2008). If PAH levels were lower than average during the sampling period, for instance, this could produce artificially low estimates of chronic risk. In future work, this uncertainty could be mitigated by sampling PAHs at multiple times throughout the year, or over the course of multiple years.

The HHRA performed in this study focuses solely on cancer as an endpoint of concern. Non-cancer endpoints such as increased asthma incidence and decreased intelligence quotient in children have been statistically correlated to PAH exposure; OPAH compounds have been shown to have potential negative impacts such as generation of ROS (Chung et al., 2006; Gale et al., 2012; Perera et al., 2009). Additionally, the air samplers used in this study only absorb PAHs in the vapor phase, omitting the particulate-bound fraction. Because the particulate-bound fraction is known to contain carcinogenic PAHs, this study's HHRA may underestimate potential carcinogenic risk associated with inhalation. The relevance of performing risk assessment using the vapor phase has been questioned due to the propensity of higher molecular weight PAHs to be in higher abundance in the particulate fraction. However, researchers have observed that the carcinogenic $B[a]P_{eq}$ can be dominated by PAHs in the vapor phase (Ramirez et al., 2011; Tsai et al., 2002). These findings provide impetus to perform risk assessments considering the vapor phase fraction of contaminants, even when data for the particulate fraction is not available.

Risk estimates presented here can be used to compare how exposure to PAH mixtures measured at different sites may affect lifetime cancer risk in humans. Importantly, they are not actual observations of cancer incidence. These risk estimates are, however, useful for comparing potential carcinogenicity among sites and through different exposure scenarios. They are also useful for prioritizing plans for remediation and mitigation. Furthermore, the estimated ELCR values associated with PAH inhalation suggest the potential for impact to other species, specifically marine mammals that respire at the air-water interface.

4.0 CONCLUSIONS

The Willamette River acted as a sink, rather than a source, for the majority of vapor phase PAHs measured in this study at sites both within and outside of the PHSM. Elevated PAH deposition rates outside the PHSM show that some contaminants measured within the PHSM may be coming from sources that are not directly related to the site's Superfund designation. An additional component of diffusive flux that should be investigated in the future is the exchange between water and sediment pore-water. This would further complete the picture of contaminant fate. Estimated ELCRs showed that chronic inhalation exposure to PAH concentrations measured within the PHSM boundaries during this study would slightly increase lifetime cancer risk. Estimated ELCRs for dermal exposure to water exceeded baseline levels of concern. Due to the short sampling period and subsequent extrapolation of the data used to estimate ELCRs, care should be taken in interpreting estimations of increased cancer risk. Estimated ELCRs are meant to enable comparison and prioritization of carcinogenic risk among different sites and through different exposure routes. The authors call for further investigation of inhalation-based risk within and around the PHSM, and at other similarly contaminated urban sites.

Supplementary Material

Refer to Web version on PubMed Central for supplementary material.

ACKNOWLEDGEMENTS

REFERENCES

Albinet A, Leoz-Garziandia E, Budzinski H, ViIlenave E. Polycyclic aromatic hydrocarbons (PAHs), nitrated PAHs and oxygenated PAHs in ambient air of the Marseilles area (South of France): Concentrations and sources. Science of The Total Environment 2007; 384: 280–292.17590415

Allan SE, Smith BW, Anderson KA. Impact of the Deepwater Horizon Oil Spill on Bioavailable Polycyclic Aromatic Hydrocarbons in Gulf of Mexico Coastal Waters. Environmental Science & Technology 2012; 46: 2033–2039.22321043

Allan SE, Sower GJ, Anderson KA. Estimating risk at a Superfund site using passive sampling devices as biological surrogates in human health risk models. Chemosphere 2011; 85: 920–927.21741671

Anderson K, Sethajintanin D, Sower G, Quarles L. Field trial and modeling of uptake rates of in situ lipid-free polyethylene membrane passive sampler. Environmental Science & Technology 2008; 42: 4486–4493.18605575

Anderson KA, Szelewski MJ, Wilson G, Quimby BD, Hoffman PD. Modified ion source triple quadrupole mass spectrometer gas chromatograph for polycyclic aromatic hydrocarbon analyses. Journal of Chromatography A 2015; 1419: 89–98.26454790

ATSDR. Public Health Assessment: Portland Harbor, Multnomah County, Oregon. In: EPA Facility ID: OR0001297969 Oregon Department of Human Services Superfund Health Investigation and Education Program UDoHaHS, Agency for Toxic Substances and Disease Registry, Atlanta, GA., editor, 2006.

ATSDR. Public Health Assessment, Final Release, Portland Harbor: Recreational Use, Portland, Oregon. U.S. Department of Health and Human Services Public Health Service, Agency for Toxic Substances and Disease Registry and Oregon Health Authority, Environmental Health Assessment Program,, 2011.

Baek S, Field R, Goldstone M, Kirk P, Lester J, Perry R. A review of atmospheric polycyclic aromatic hydrocarbons: sources, fate and behavior. Water, Air, & Soil Pollution 1991; 60: 279–300.

Baker JE, Eisenreich SJ. Concentrations and fluxes of polycyclic aromatic hydrocarbons and polychlorinated biphenyls across the air-water interface of Lake Superior. Environmental Science & Technology 1990; 24: 342–352.

Bamford HA, Offenberg JH, Larsen RK, Ko FC, Baker JE. Diffusive exchange of polycyclic aromatic hydrocarbons across the air-water interface of the Patapsco River, an urbanized subestuary of the Chesapeake Bay. Environmental Science & Technology 1999a; 33: 2138–2144.

Bamford HA, Poster DIL, Baker JE. Temperature dependence of Henry's law constants of thirteen polycyclic aromatic hydrocarbons between 4 C and 31 C. Environmental Toxicology and Chemistry 1999b; 18: 1905–1912.

Bartkow ME, Huckins JN, Müller JF. Field-based evaluation of semipermeable membrane devices (SPMDs) as passive air samplers of polyaromatic hydrocarbons (PAHs). Atmospheric Environment 2004; 38: 5983–5990.

Bartkow ME, Jones KC, Kennedy KE, Holling N, Hawker DW, Müller JF. Evaluation of performance reference compounds in polyethylene-based passive air samplers. Environmental Pollution 2006; 144: 365–370.16631287

Booij K, Smedes F. An improved method for estimating in situ sampling rates of nonpolar passive samplers. Environmental Science & Technology 2010; 44: 6789–6794.20701278

Chung MY, Lazaro RA, Lim D, Jackson J, Lyon J, Rendulic D, Aerosol-borne quinones and reactive oxygen species generation by particulate matter extracts. Environmental Science & Technology 2006; 40: 4880–4886.16955881

Daisey J, Leyko M, Kneip T. Source identification and allocation of polynuclear aromatic hydrocarbon compounds in the New York City aerosol: methods and applications. Polynuclear Aromatic Hydrocarbons. Ann Arbor Science, Ann Arbor 1979: 201–215.

Donald CE, Elie MR, Smith BW, Hoffman PD, Anderson KA. Transport stability of pesticides and PAHs sequestered in polyethylene passive sampling devices. Environmental Science and Pollution Research 2016: 1–8.26728290

EPA. Portland Harbor Superfund Site. 2015 EPA, 2015.

EPA US. Guidelines for Carcinogen Risk Assessment, Washington, D.C., 2005.

EPA US. Development of a Relative Potency Factor (RPF) Approach for Polycyclic Aromatic Hydrocarbon (PAH) Mixtures Intregrated Risk Information Systems (IRIS), Washington, D.C., 2010.

EPA US. Memo: Recommended Default Exposure Factors Office of Solid Waste and Emergency Response, Washington, D.C., 2014.

Esen F, Tasdemir Y, Vardar N. Atmospheric concentrations of PAHs, their possible sources and gas-to-particle partitioning at a residential site of Bursa, Turkey. Atmospheric Research 2008; 88: 243–255.

Fang M-D, Lee C-L, Jiang J-J, Ko F-C, Baker JE. Diffusive exchange of PAHs across the air-water interface of the Kaohsiung Harbor lagoon, Taiwan. Journal of Environmental Management 2012; 110: 179–187.22789653

Galarneau E Source specificity and atmospheric processing of airborne PAHs: implications for source apportionment. Atmospheric Environment 2008; 42: 8139–8149.

Gale SL, Noth EM, Mann J, Balmes J, Hammond SK, Tager IB. Polycyclic aromatic hydrocarbon exposure and wheeze in a cohort of children with asthma in Fresno, CA. Journal of Exposure Science and Environmental Epidemiology 2012; 22: 386–392.22549720

Gevao B, Hamilton-Taylor J, Jones KC. Polychlorinated biphenyl and polycyclic aromatic hydrocarbon deposition to and exchange at the air-water interface of Esthwaite Water, a small lake in Cumbria, UK. Environmental Pollution 1998; 102: 63–75.

Greenberg MS, Chapman PM, Allan IJ, Anderson KA, Apitz SE, Beegan C, Passive sampling methods for contaminated sediments: Risk assessment and management. Integrated environmental assessment and management 2014; 10: 224–236.24343931

Gustafson KE, Dickhut RM. Gaseous exchange of polycyclic aromatic hydrocarbons across the air-water interface of southern Chesapeake Bay. Environmental Science & Technology 1997; 31: 1623–1629.

Howsam M, Jones KC. Sources of PAHs in the environment PAHs and related compounds. Springer, 1998, pp. 137–174.

Huckins JN, Petty JD, Booij K. Monitors of organic chemicals in the environment: semipermeable membrane devices: Springer New York, 2006.

Huckins JN, Petty JD, Lebo JA, Almeida FV, Booij K, Alvarez DA, Development of the permeability/ performance reference compound approach for in situ calibration of semipermeable membrane devices. Environmental Science & Technology 2002; 36: 85–91.11811495

Jakober CA, Riddle SG, Robert MA, Destaillats H, Charles MJ, Green PG, Quinone emissions from gasoline and diesel motor vehicles. Environmental Science & Technology 2007; 41: 4548–4554.17695895

Johnson M A numerical scheme to calculate temperature and salinity dependent air-water transfer velocities for any gas. Ocean Sci 2010; 6: 913–932.

Khairy MA, Lohmann R. Field validation of polyethylene passive air samplers for parent and alkylated PAHs in Alexandria, Egypt. Environmental Science & Technology 2012; 46: 3990–3998.22397460

Knecht AL, Goodale BC, Truong L, Simonich MT, Swanson AJ, Matzke MM, Comparative developmental toxicity of environmentally relevant oxygenated PAHs. Toxicology and applied pharmacology 2013; 271: 266–275.23684558

Li J, Cheng H, Zhang G, Qi S, Li X. Polycyclic aromatic hydrocarbon (PAH) deposition to and exchange at the air-water interface of Luhu, an urban lake in Guangzhou, China. Environmental Pollution 2009; 157: 273–279.18692286

Lohmann R, Dapsis M, Morgan EJ, Dekany V, Luey PJ. Determining air-water exchange, spatial and temporal trends of freely dissolved PAHs in an urban estuary using passive polyethylene samplers. Environmental Science & Technology 2011; 45: 2655–2662.21351793

Lohmann R, Klanova J, Kukucka P, Yonis S, Bollinger K. Concentrations, fluxes, and residence time of PBDEs across the tropical Atlantic Ocean. Environmental Science & Technology 2013; 47: 13967–13975.24224767

Lundstedt S, White PA, Lemieux CL, Lynes KD, Lambert IB, Öberg L, Sources, fate, and toxic hazards of oxygenated polycyclic aromatic hydrocarbons (PAHs) at PAH-contaminated sites. AMBIO: A Journal of the Human Environment 2007; 36: 475–485.

Mallakin A, Dixon DG, Greenberg BM. Pathway of anthracene modification under simulated solar radiation. Chemosphere 2000; 40: 1435–1441.10789985

Matzke MM, Allan SE, Anderson KA, Waters KM. An approach for calculating a confidence interval from a single aquatic sample for monitoring hydrophobic organic contaminants. Environmental Toxicology and Chemistry 2012; 31: 2888–2892.22997050

McDonough CA, Khairy MA, Muir DC, Lohmann R. The significance of population centers as sources of gaseous and dissolved PAHs in the lower Great Lakes. Environmental Science & Technology 2014; 48: 7789–7797.24918966

Morgan EJ, Lohmann R. Detecting air-water and surface-deep water gradients of PCBs using polyethylene passive samplers. Environmental Science & Technology 2008; 42: 7248–7253.18939554

Nelson ED, McConnell LL, Baker JE. Diffusive exchange of gaseous polycyclic aromatic hydrocarbons and polychlorinated biphenyls across the air-water interface of the Chesapeake Bay. Environmental Science & Technology 1998; 32: 912–919.

Nielsen T Traffic contribution of polycyclic aromatic hydrocarbons in the center of a large city. Atmospheric Environment 1996; 30: 3481–3490.

O'Connell SG, McCartney MA, Paulik LB, Allan SE, Tidwell LG, Wilson G, Improvements in pollutant monitoring: Optimizing silicone for co-deployment with polyethylene passive sampling devices. Environmental Pollution 2014; 193: 71–78.25009960

Paulik LB, Donald CE, Smith BW, Tidwell LG, Hobbie KA, Kincl L, Emissions of Polycyclic Aromatic Hydrocarbons from Natural Gas Extraction into Air. Environmental Science & Technology 2016a; 50: 7921–7929.27400263

Paulik LB, Donald CE, Smith BW, Tidwell LG, Hobbie KA, Kincl L, PAH emissions from natural gas extraction into air. Environmental Science & Technology 2016b; 10.1221/acs.est.6b02762.

Perera FP, Li Z, Whyatt R, Hoepner L, Wang S, Camann D, Prenatal airborne polycyclic aromatic hydrocarbon exposure and child IQ at age 5 years. Pediatrics 2009; 124: el95–e202.

Phillips DH. Fifty years of benzo(a)pyrene. Nature 1983; 303: 468–472.6304528

Pies C, Hoffmann B, Petrowsky J, Yang Y, Ternes TA, Hofmann T. Characterization and source identification of polycyclic aromatic hydrocarbons (PAHs) in river bank soils. Chemosphere 2008; 72: 1594–1601.18513782

Prest HF, Huckins JN, Petty JD, Herve S, Paasivirta J, Heinonen P. A survey of recent results in passive sampling of water and air by semipermeable membrane devices. Marine pollution bulletin 1995; 31: 306–312.

Ramirez N, Cuadras A, Rovira E, Marcé RM, Borrull F. Risk assessment related to atmospheric polycyclic aromatic hydrocarbons in gas and particle phases near industrial sites. Environmental health perspectives 2011; 119: 1110.21478082

Schwarzenbach RP, Gschwend PM, Imboden DM. Environmental organic chemistry: Wiley-Interscience, 2002.

Selifonov SA, Grifoll M, Eaton RW, Chapman PJ. Oxidation of naphthenoaromatic and methyl-substituted aromatic compounds by naphthalene 1, 2-dioxygenase. Applied and environmental microbiology 1996; 62: 507–514.16535238

Sen S, Field JM. Genotoxicity of polycyclic aromatic hydrocarbon metabolities: radical cations and ketones. Adv Mol Toxicol. 7, 2013, pp. 83–127.

Shen G, Tao S, Wang W, Yang Y, Ding J, Xue M, Emission of oxygenated polycyclic aromatic hydrocarbons from indoor solid fuel combustion. Environmental Science & Technology 2011; 45: 3459–3465.21375317

Sower GJ, Anderson KA. Spatial and temporal variation of freely dissolved polycyclic aromatic hydrocarbons in an urban river undergoing superfund remediation. Environmental Science & Technology 2008; 42: 9065–9071.19174872

Tidwell LG, Allan SE, O'Connell SG, Hobbie KA, Smith BW, Anderson KA. PAH and OPAH flux during the Deepwater Horizon incident. Environmental Science & Technology 2016; 50: 7489–7497.27391856

Tobiszewski M, Namiesnik J. PAH diagnostic ratios for the identification of pollution emission sources. Environmental Pollution 2012; 162: 110–119.22243855

Tsai P-J, Shieh H-Y, Lee W-J, Lai S-O. Characterization of PAHs in the atmosphere of carbon black manufacturing workplaces. Journal of hazardous materials 2002; 91: 25–42.11900904

Vorhees DJ, Cullen AC, Altshul LM. Exposure to polychlorinated biphenyls in residential indoor air and outdoor air near a Superfund site. Environmental Science & Technology 1997; 31: 3612–3618.

Westbrook CK, Pitz WJ, Curran HJ. Chemical kinetic modeling study of the effects of oxygenated hydrocarbons on soot emissions from diesel engines. The Journal of Physical Chemistry A 2006; 110: 6912–6922.16722706

WHO. Air quality guidelines for Europe. World Health Organization Regional Office for Europe, Copenhagen, Denmark, 2000.

Yunker MB, Macdonald RW, Vingarzan R, Mitchell RH, Goyette D, Sylvestre S. PAHs in the Fraser River basin: a critical appraisal of PAH ratios as indicators of PAH source and composition. Organic Geochemistry 2002; 33: 489–515.

Zhang W, Zhang S, Wan C, Yue D, Ye Y, Wang X. Source diagnostics of polycyclic aromatic hydrocarbons in urban road runoff, dust, rain and canopy throughfall. Environmental Pollution 2008; 153: 594–601.17949873

Highlights:

- Superfund sites are suspected sources of risk-driving PAH air pollution

- Passive air and water samplers enable quantitative PAH and OPAH flux assessment

- The Portland Harbor Superfund Mega-site is an air pollutant sink, not a source

- PAH deposition was greatest at a site upriver of the Superfund site

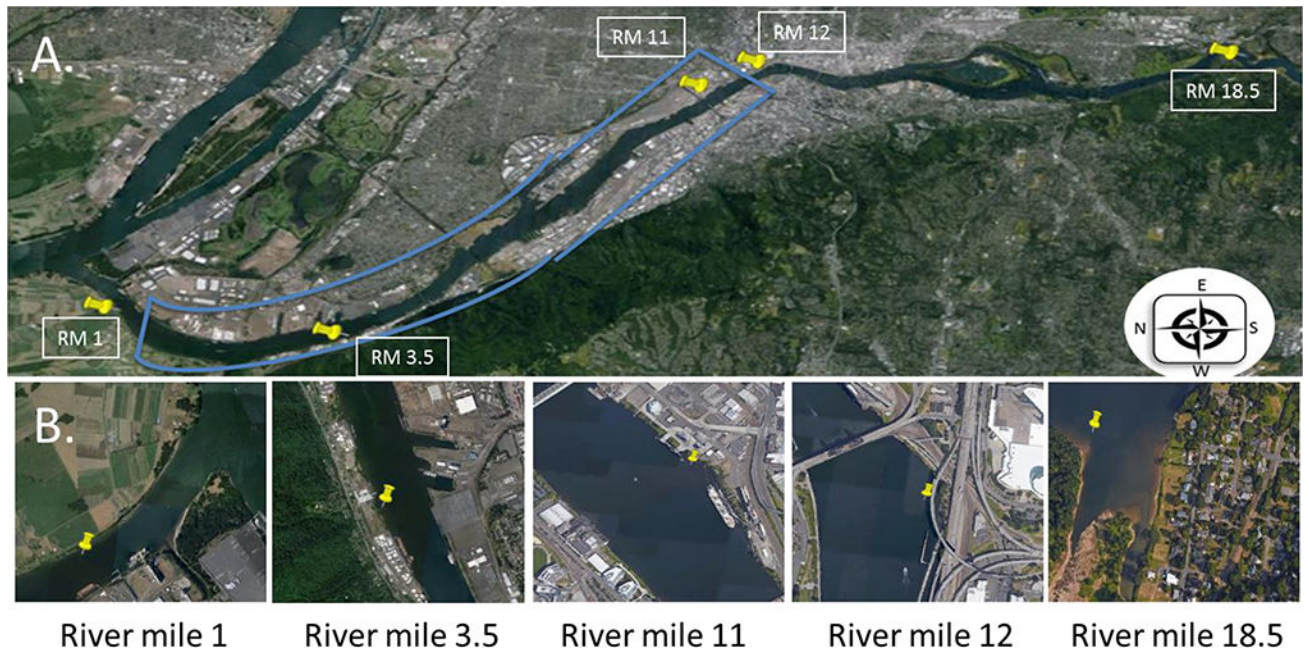- Inhaling PAHs measured in the Superfund increases estimated cancer risk

Figure 1:
A: Willamette river from river mile 20 to the confluence of the Willamette and the Columbia. Blue box designates Portland Harbor Superfund study area from river mile 1.9 to river mile 11.8. Yellow pins designate sampling sites. B: Close up sections of each sampling site. River mile 1 adjacent to agricultural lands, river mile 3.5 and 11 located within the Superfund, river mile 12 located in highly urbanized region, river mile 18.5 located near residential region.
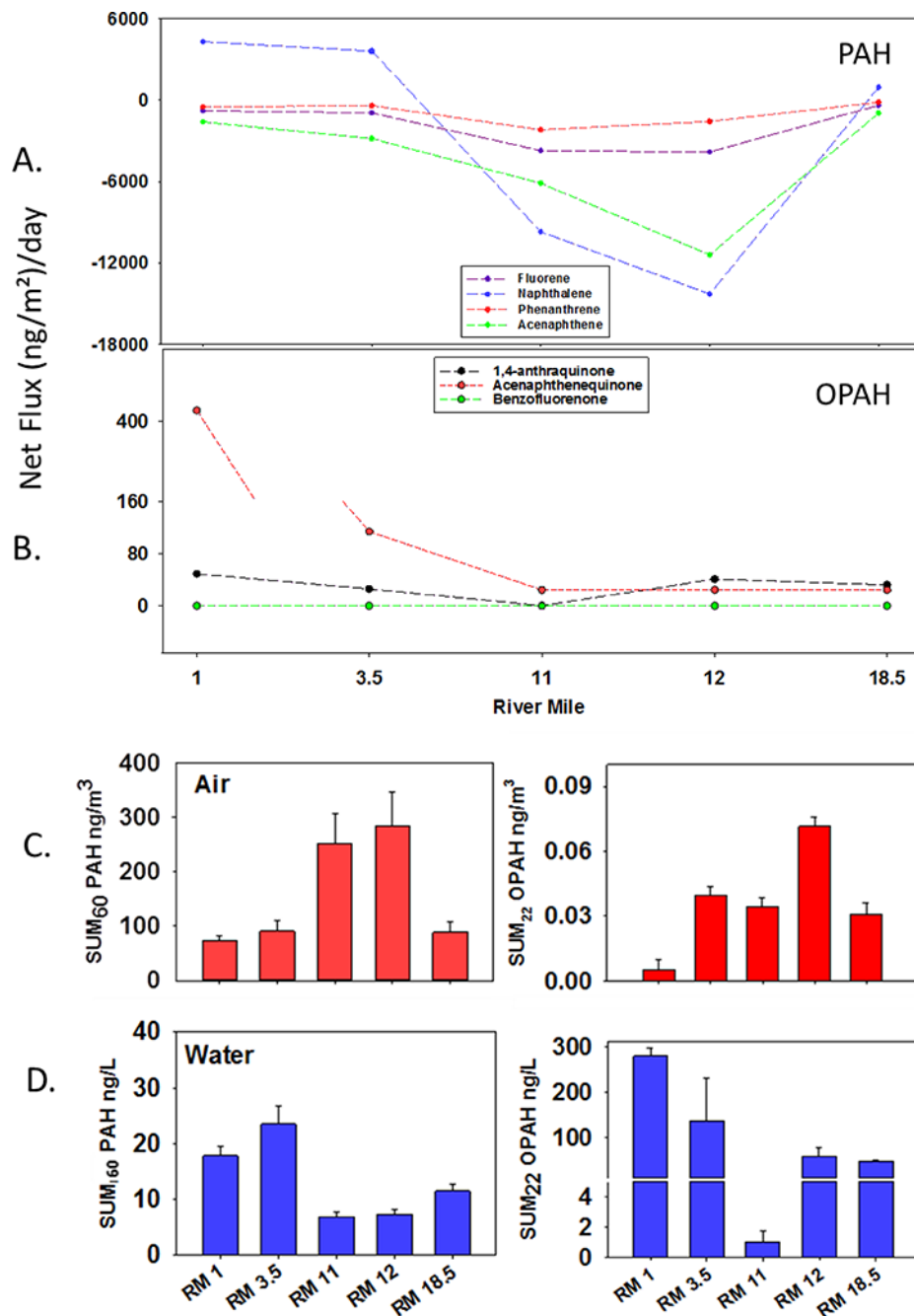
Figure 2:
A: Four PAHs that had the greatest mass transfer across the superfund. Naphthalene had the greatest deposition of all PAH. B: Flux of three OPAHs that resulted in the greatest mass transfer. C: $\Sigma 60$ PAHs and $\Sigma 22$ OPAHs in air. D: Σ_{60} PAHs and Σ_{22} OPAHs in water. Error bars represent 95% confidence interval calculated from N=3 replicates at two sites and applied to the other sites.
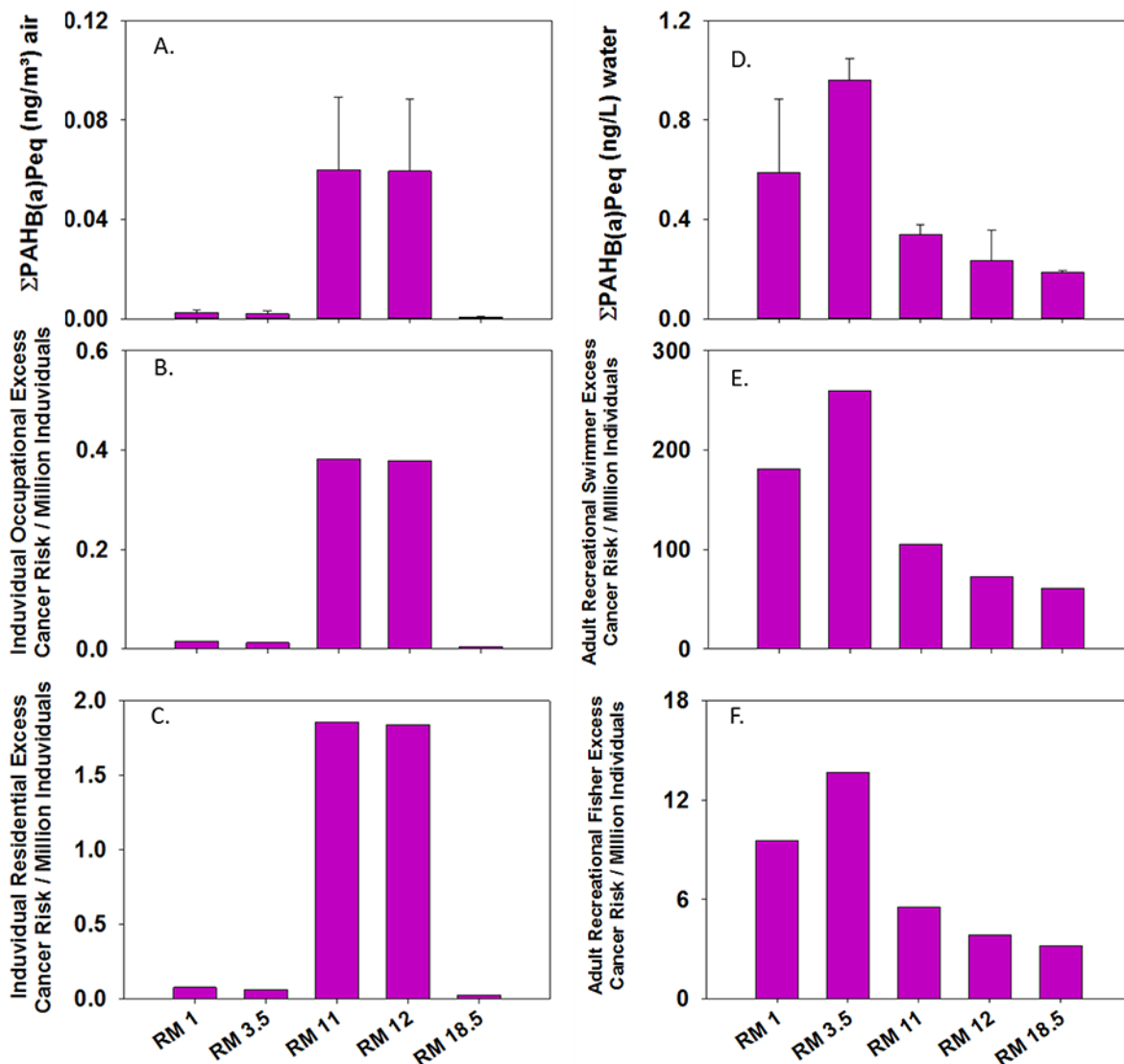
Figure 3:
A: Carcinogenic potency in benzo[a]pyrene equivalence of PAHs measured in air at each river mile. Error bars represent 95% confidence interval calculated from N=3 replicates at two sites and applied to the other sites. B: Number of individuals exceeding the 1 in 1 million level of concern using an occupational inhalation ELCR. C: Number of individuals exceeding the 1 in 1 million level of concern using a residential inhalation ELCR. D: Carcinogenic potency in benzo[a]pyrene equivalence of PAHs measured in water at each river mile. Error bars represent 95% confidence interval calculated from N=3 replicates at two sites and applied to the other sites. E: Number of individuals exceeding the 1 in 1 million level of concern using a dermal exposure recreational swimmer ELCR. F: Number of individuals exceeding the 1 in 1 million level of concern using a recreational fisher person dermal exposure ELCR.